Sustainable Design from Waste Up: Irradiated Graphite Disposal Assessments to Inform Reactor Design and Operation

Liam Hines[a,1], Haruko Wainwright[a], Craig Benson[b], Lance L Snead [c,d], Anthony J. Wickham [e]

[a] *Department of Nuclear Science and Engineering, Massachusetts Institute of Technology, 77 Massachusetts Ave, Cambridge MA 02140*

[b] *Department of Civil and Environmental Engineering, University of Wisconsin-Madison, 1415 Engineering Drive Madison, WI 53706*

[c] *Nuclear Reactor Laboratory, Massachusetts Institute of Technology, 77 Massachusetts Ave, Cambridge MA 02140*

[d] *Materials Science and Chemical Engineering, Stony Brook University, Stony Brook NY 11794*

[e] *Nuclear Technology Consultancy, Laugharne SA33 4QL, UK.*

[1] *Corresponding author. Email: LSHines@mit.edu Tel.: +1 203 892 1962.*

As Gen IV graphite-moderated reactor technologies advance to demonstration and deployment, the question must be answered of how, where, and when to dispose of the irradiated graphite waste produced from the operation of these facilities. This work presents an integrated assessment involving the entire graphite lifecycle in nuclear power production: impurity measurement of graphite grades, reactor simulations for source-term characterization, and repository simulations for subsurface radionuclide transport from a hypothetical near-surface low-level waste repository. This integration enables the feedback from the disposal assessment to evaluate the engineering design parameters. We demonstrate our approach based on a hypothetical repository with hydrogeological parameters representative of the arid western region in the US. Our results show that mobile carbon-14 is the largest contributor to radioactivity and offsite groundwater concentrations, and that crediting a graphite waste form reduces the concentrations significantly, since it limits the radionuclide release. The sensitivity analysis then shows the dominant impact of release rates from the waste forms compared to sorption and other transport parameters. In addition, reduced-order models are developed separately for the reactor model and repository model to combine two models in a modular structure, and to explore the acceptable nitrogen impurity and operational period for satisfying the repository criteria. The framework developed in this study enables us to quantify the risks associated with the disposal of major radioactive waste streams from advanced reactors, and to consider such characteristics in the reactor engineering designs.

Keywords: Low Level Radioactive Waste, Waste Management, Performance Assessment, Irradiated Graphite, High Temperature Gas Reactor

1. Introduction

As Generation IV reactor concepts approach demonstration, solving practical challenges related to construction, operation, and decommissioning is essential for successful deployment. One challenge posed is the management of irradiated graphite produced by reactor designs including high temperature gas reactors (HTGRs) and fluoride-cooled high-temperature reactors (FHRs). For these reactor designs, graphite serves not only as a neutron moderator but as a robust structural material capable of operating at high temperatures. The performance of graphite at high temperatures not only increases thermal efficiency and opens access to higher temperature heat applications, but also provides wide safety margins during accident scenarios that could cause fuel failure [1]. However, the irradiation of graphite structures during the operation of these reactors produces a number of radioactive species, most notably C-14, with a half-life of 5730 years. Recently, Hines et al. [2] showed that graphite constitutes the largest component of graphite-moderated reactor designs in decommissioning, accounting for more than 80% of the core volume and up to 14% of the disposal costs for some designs [2,3].

In fact, there are currently about 55,000 metric tons of legacy irradiated graphite waste managed or disposed of in the US. A majority of this waste was produced in research reactors or weapons production facilities [4]. Some of the most recent US experience in managing large volumes of irradiated graphite involved the decommissioning of the Brookhaven Graphite Research Reactor. While the research reactor ceased operation in 1968, work to dismantle the 700 metric tons of graphite moderator and reflector did not begin until 2009 with all graphite removed from the site and transported to the US Department of Energy's Nevada Test Site by 2010 [4].

The remaining graphite waste handled by the commercial nuclear industry has been the product of two relatively short-lived graphite moderated, gas-cooled reactors: Peach Bottom Unit I and Fort St. Vrain [5,6]. For this small inventory of commercial irradiated graphite waste, some of the inventory has been placed in temporary or onsite storage, while the Fort St. Vrain plant has been decommissioned and its irradiated graphite disposed of in one of the low-level radioactive waste (LLW) disposal sites in Richland, WA [5,7]. While these past graphite management strategies have been satisfactory for the relatively low volumes of irradiated graphite managed by commercial enterprises, the volume of graphite managed in the US could grow by upwards of 60,000 tons over the next several decades [2]. A comprehensive approach will be necessary moving forward to support the effective and economic deployment of advanced graphite-moderated reactor designs.

Managing graphite waste requires an understanding of radioactive waste disposal regulations. Particular attention is paid to US radioactive waste regulation as a case study for how specific classification criteria can impact the manageability of waste streams without entirely capturing the associated risks. In the US, the LLW facilities currently use the waste acceptance criteria (WAC) outlined in the requirements for radioactive waste repositories outlined 10 CFR 61 [8]. The waste classes defined in 10 CFR 61 are all considered Low Level Waste in the US, but these same criteria span the classifications of Low Level Waste and Intermediate Level Waste as defined by the International Atomic Energy Agency [F]. For the US system, waste classifications are based on prescriptive activity concentrations for specific radionuclides. The activity limits are defined for three classes of waste: Class A, the least restrictive radioactive waste classification; Class B, radioactive waste containing a considerable inventory of short-lived radionuclides that warrants special concern for short-term stability; and Class C, radioactive waste containing a considerable inventory of long-lived radionuclides that warrant special concern for long-term isolation beyond the credited institutional control of the near-surface repository. Radioactive waste that exceeds Class C thresholds is designated Greater than Class C (GTCC) and is considered not suitable for shallow disposal [8]. Previous efforts to characterize the irradiated waste produced by the operation of Gen IV reactor designs indicate that most graphite would be classified as Class C or GTCC in the US and as Intermediate Level Waste in most other classification schemes, primarily because of the large inventories of C-14 [2, G].

The waste classifications are the result of pathways analyses, considering how radionuclides from a disposal facility could transport to a human receptor in a number of offsite exposure and intrusion scenarios [9]. The WAC for a given radionuclide is determined by the lowest concentration capable of exceeding the public health objective of 25 mrem/year in any exposure or intrusion scenario. For each radionuclide analyzed in 10 CFR 61, the limiting exposure event was an inadvertent intruder scenario, where some person becomes exposed to disposed radioactive wastes by working or living on the waste site after lapse of the 100-year institutional

control period [9]. While scenarios of offsite migration of radionuclides, including groundwater infiltration, are considered, these scenarios were calculated to have lower health impacts compared to inadvertent intrusion.

In addition, the classifications are based on simplifying assumptions through the pathways analyses, which allow the generic application of WAC for any waste disposed of at any waste site. However, the pathways analyses do not consider any packages or waste forms to potentially contain radionuclides other than metal. In the case of the intrusion scenario, it was assumed that an intruder would recognize long-term stable wastes (such as metal) and stop excavation within six hours, while they would not recognize other degraded waste forms and continue excavation. The result is less restrictive radionuclide concentration limits for activated metals, 10 times greater than other materials, justified upon the assumption of their long-term stability, and thereby, recognizability to an inadvertent intruder [9]. However, other stable waste forms, such as graphite, have not been considered or credited in the current regulations.

One opportunity to address the challenges posed by the disposal of irradiated graphite waste is recent rulemaking pursued by the Nuclear Regulatory Commission regarding LLW. The rulemaking would promote an existing provision in 10 CFR 61.58 that allows for alternative waste classifications [8]. In effect, the new rulemaking would allow LLW facilities to conduct site-specific analyses to produce their own WAC for delivered waste packages [10]. This has a significant impact on graphite waste management in two ways. First, it allows the assessment to credit the graphite waste form. Instead of modeling radionuclides in disposed wastes as immediately available for transport, the radionuclide inventory would be modeled as initially immobile with a fraction of the total inventory mobilized from the waste over time through mechanisms including radionuclide leaching from the waste form and material degradation specific to the waste form via processes including oxidation and corrosion. Graphite can exist in stable geologic formations for 1.8–2.2 billion years [11]. The release of radionuclides from graphite could therefore be significantly less than those predicted by a model agnostic to waste form that assumes immediate total availability of radionuclides in the waste. One goal of this study is to develop a method for how the robustness of graphite as a material can be incorporated into technical analyses that evaluate the safety of radioactive waste disposal. Second, risk-based approaches recognize the importance of low-consequence but more likely events, rather than extreme low-probability events. Groundwater pathways have been considered as the primary pathway of exposure to radionuclides, in more recent decisions from regulators regarding the disposal of spent nuclear fuel [12]. Similarly, regulators of industrial hazardous waste disposal sites have emphasized offsite transport of contaminants as a primary concern for long-term disposal [13]. While the intrusion scenario predicts a greater exposure, the event is much less likely to happen compared to an exposure through migration of radionuclides to a groundwater well [9].

The objective of this paper is to demonstrate a site-specific graphite disposal assessment, modeling the radionuclide transport through groundwater, and quantifying the offsite consequences. The source term—i.e., the graphite mass and radionuclide concentration—is quantified by Hines et al. [2], considering the operation of Gen IV graphite-moderated designs with the impurity concentrations of modern graphite grades [2,14]. We use hypothetical site-specific geological and repository designs representative of a low-level waste repository in the Western US. We then perform comprehensive uncertainty quantification and sensitivity analysis given the uncertainty in geological parameters and radionuclide release rates. If the consequences of disposed graphite waste in a shallow subsurface can be demonstrated to pose sufficiently low risk (defined as Class A), the site-specific WAC could offer a potential avenue to significantly reduce disposal costs of irradiated graphite.

In addition, the direct connection between the source-term calculation and disposal assessment enables feedback from the repository criteria to inform the graphite design parameters. In particular, we demonstrate the methodology to define the operation period and acceptable impurity concentrations that can satisfy WAC. The large amount of irradiated graphite—currently without disposal pathways—across the world resulted from the past operations without considering decommissioning and disposal. Custodians of large irradiated graphite inventories have found that the plans for managing the waste stream are not sufficient for the reality of the challenge, exemplified by the UK's Nuclear Restoration Services investigation of alternatives to the costly solution of disposing irradiated graphite in a non-existent geological disposal facility. Our methodology defines the material and design conditions, so that future graphite-reliant nuclear reactors can be more easily decommissioned and disposed of before any waste is produced. More broadly, the study offers a framework for sustainable development of any future energy and industrial system, where considerations of hazardous and radioactive material management are included from project inception.

2. Methods

2.1 Reactor Model for Source-term Characterization

The radionuclide source inventory in the graphite is calculated in Hines et al. based on the simulated activation of a graphite-moderated high temperature gas reactor [2]. We briefly summarize the model for completeness. We assume a hypothetical Modular High Temperature Gas Reactor (MHTGR), a 350 MWth graphite-moderated reactor designed by General Atomics and benchmarked by several US national labs [15]. The MHTGR core is modeled with a simplified radially symmetrical geometry consisting of 10 concentric cylinders: three inner graphite reflector rings, three homogenized fueled rings, and four outer reflector rings. The Monte Carlo neutron transport code MCNPX, coupled with the CINDER90 transmutation package, is used to simulate 20 years of full power operation and 15 years of decay before graphite disposal. The volume average radionuclide concentration is calculated for the 220 m^3 graphite reflector to produce a single source concentration for the tracked radionuclides.

We analyzed several grades of graphite, both historical graphite used in past nuclear applications including the Hanford B-reactor and the Windscale prototype Advanced Gas Reactor, as well as modern industrial and nuclear-qualified graphite compositions (ETU-10, ET-10, IG-110). While historical graphite compositions are not under consideration for new nuclear projects, they are included in the analysis to increase the range of inputs to examine output sensitivity on nitrogen impurity. For ease of comparison, a constant graphite density of 1.75 g/cm^3 is modeled for each graphite grade, resulting in a constant graphite mass of 390 MT and surface area of 180 m^2, although density can vary between grades [14]. The difference between graphite grades is captured in the reactor model as a difference in impurities in the modeled graphite isotopic composition of the reflector regions [2, 14]. The most important impurity for this study is nitrogen, one of the dominant precursors in addition to C-13 in the bulk carbon that produce C-14 when irradiated [2]. One goal for the study of differing impurity contents of graphite grades is to determine the relative contributions from N-14 and C-13 activation to the total C-14 inventory of a reference high temperature gas reactor. A summary of the graphite grades simulated, the associated nitrogen impurities, and the resulting C-14 source term are presented in Table 1 [2,14].

Table 1. Nitrogen impurity content in the original graphite and resulting C-14 concentration in graphite waste of several graphite compositions following simulated operation of 20 years in Modular High Temperature Gas Reactor. The simulation was done by Hines et al. [2,14].

Graphite Grade/Source	**N Impurity [appm]**	**C-14 Concentration [Ci/m^3] Simulated by Hines et al. [2]**
ETU-10	4.87	3.19
ET-10	3.52	2.60
IG-110	2.65	2.37
Windscale AGR	10.6	7.17
Hanford B-Reactor	31.0	16.8

2.2 Repository Assessment Models

To calculate the consequences of irradiated graphite disposal in a LLW repository, we develop a radionuclide transport model based on the performance assessment of a reference repository in the arid Western US [16, 17]. A schematic diagram of the repository and dominant transport mechanisms is depicted in Figure 1. The reference site is composed of an embankment filled with silt backfill and covered with a clay radon barrier, filter material, and an erosion protection layer. Below the disposed waste is a clay liner followed by an unsaturated zone composed of silt and a saturated zone composed of sand. A hypothetical groundwater well is assumed at the site boundary 73 meters downstream of the region beneath the waste [17].

The repository performance assessment model is developed using Goldsim, software commonly used for repository performance assessments [17]. Goldsim is a Monte Carlo simulation software with particular capabilities for modeling solute transport in porous media. One strength of Goldsim lies in extensive uncertainty quantification capabilities necessary to evaluate the repository performance impacted by highly uncertain parameters, including radionuclide inventory, hydrogeological parameters, and climate variables [18]. While multiple exposure and transport pathways were considered for the original assessment (10 CFR 61), this study considers only the subsurface water intrusion and gaseous diffusion pathways.

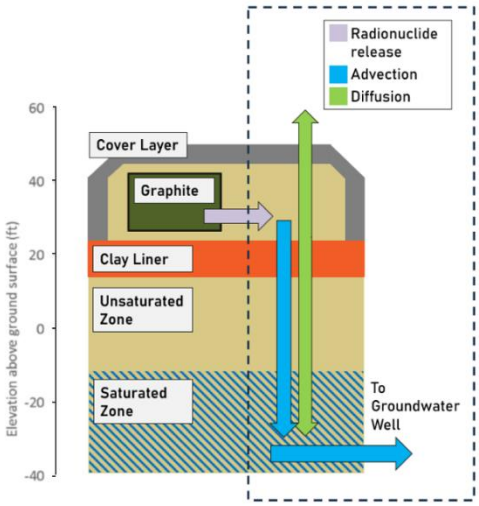

Figure 1. Conceptual model of the LLW repository performance assessment. Graphite degradation is modeled by adding the radionuclide inventory at a constant rate to a 1-dimensional transport model from the graphite waste form to the soil outside. The 1-dimensional transport model incudes advection downward (through a clay liner below the site and a silt-filled unsaturated zone) into a groundwater aquifer composed of sand where species are then transported laterally to a groundwater well. Transport of gaseous species including C-14 as CO2 is additionally modeled upwards through diffusion.

The infiltration and vertical flow are modeled in a one-dimensional (1D) domain via a first-order numerical solution to the Darcy flow equation [17], while the saturated zone flow is 1D horizontal. Representative soil classes and hydrological parameters are assigned to each material for the waste material, clay liner, unsaturated zone and saturated zone. Details of the site geology and hydrological model are discussed in Appendix A.

The transport of radionuclides is then modeled via advection-diffusion in the saturated and unsaturated media of the waste site. Goldsim includes a numerical solver for advection-diffusion with the finite element method. For each radionuclide, the most mobile chemical species in groundwater is selected, which supports conservative estimation of consequences from offsite transport [19]. The most important mechanism modeled to impact the advective transport of radionuclides is sorption. Sorption describes the partitioning of chemical species out of a solvent to form surface complexes. In the case of groundwater transport, the relative high surface-area of soil pores can significantly retard the transport of dissolved radionuclides through sorption. Sorption is modeled in the study's radionuclide transport model as the parameter K_d, which is the ratio of the mass of a species sorbed as a surface complex to the mass of a species dissolved in the transport fluid [20].

The modeled radionuclide inventory for the reference graphite grade ETU-10, as well as the selected chemical species, are described in Table 2. In addition to C-14, three other radionuclides are analyzed through the model: H-3, Cl-36, and Ni-63. H-3 was selected for analysis due to its impact as the second greatest contributor to total radioactivity in irradiated reflector graphite in previous work [2]. Cl-36 was selected for analysis due to its potential high mobility that could drive calculated offsite radionuclide concentrations despite its low initial inventory. Ni-63 was chosen as a comparison case, as it was calculated to contribute a similar fraction of total radioactivity in graphite as Cl-36 but is modeled to be less mobile in groundwater compared to C-14 and Cl-36. For C-14 and H-3, we assume that the selected chemical species are oxidized species, since the repository is in an oxic condition near surface above the water table. For Cl-36 and Ni-63, the chemical species selected is the elemental ion. In reality, each of the radionuclides analyzes, particularly C-14 and Cl-36, will be present as a number of chemical species. In the case of C-14, the production route, whether from activation of N-14 or C-13, will impact its chemical form within the graphite material and the potential mechanisms for mobilization from the graphite and specific chemical species the C-14 will take once mobilized. The selected

species represent a worst-case scenario where each radionuclide is the most mobile in the groundwater environment.

The release rate of radionuclides from the graphite waste form is defined in the 1-D transport model to represent the release from the graphite to the surrounding soil, defined by a constant fraction of the radionuclide inventory released at each computed time step. The release rate is chosen to offer some credit to the waste form of graphite, while allowing for large uncertainty in how exactly the graphite will perform over long periods of time.

Radionuclide transport in the repository model is simulated for 10,000 years, and the peak concentrations for each radionuclide are computed at the offsite groundwater well. The concentration of radionuclides in the groundwater well are compared against the ground water protection limits (GWPL), radionuclide concentrations that would result in doses in excess of 4 mrem, 0.04 mSv, per year from ingesting the groundwater [16, 27]. The study's repository model is benchmarked against the performance assessment of depleted uranium disposal that it was developed from by calculating the peak concentration of two key radionuclides. Further details on the benchmarking are discussed in Appendix B.

Table 2. Radionuclide inventory from simulated activation of ETU-10 graphite and modeled species for performance assessment

Radionuclide	**Half-Life [years]**	**Source Concentration [Ci/m3]**	**Release Rate (min, max) [1/yr]**	**Chemical Species**
H-3	1.23E1	2.39E0	2.94E-19, 2.30E-2	HTO
C-14	5.73E3	3.19E0	1.18E-15, 3.29E-4	CO_2
Cl-36	3.01E5	2.12E-1	9.29E-16, 1.10E-2	Cl^-
Ni-63	1.00E2	5.21E-1	1.34E-19, 1.91E-7	Ni^{2+}

2.3 Uncertainty Quantification in the Repository Assessment

We have compiled the reference site parameters as well as literature values to quantify the parameter uncertainty in the repository assessment. Radionuclide release-rate is modeled as a log-uniform distribution between the minimum and maximum value (Table 4) according to the formula:

$$P(X) = \frac{1}{X(ln\frac{max}{min})}$$

Where P(X) is the probability of sampling point X, *max* is the largest literature value reviewed for the particular radionuclide release-rate, and *min* is the correspondingly smallest literature value reviewed. The log-uniform distribution was selected due to the wide range of values for radionuclide release: over 10 orders of magnitude for each radionuclide, and for the uncertainty in the sampling method for leach-rate values: values were selected from leach-rate studies and theoretical models of graphite oxidation with an equal weighting for the viability of each value. The final log-uniform distribution takes as inputs on the minimum and maximum surveyed values and assigns equal probability over each order of magnitude [17]. Note that log-uniform distributions have been typically used for representing parameter uncertainty, particularly when the range spans several orders of magnitudes [12, 17].

The minimum release rate for each radionuclide is determined by the estimated oxidation rate of graphite in aqueous conditions developed for the performance assessment of TRISO fuel disposed in Yucca Mountain, which has similar geochemical conditions (oxidizing) to the reference site [17, 21]. The release rate for a particular radionuclide is then calculated assuming the congruent release of that radionuclide with the graphite degradation. Maximum release rate for each radionuclide is selected from the literature of measured leach-rate during radionuclide leaching experiments of irradiated graphite [22, 29]. We note here that the graphite

leaching studies reviewed for radionuclide release-rate include irradiated graphite samples that will significantly differ in operational environment compared to graphite components in Generation IV advanced nuclear systems. In particular, the maximum values for C-14 and Cl-36 leaching are derived from a leach study of RBMK graphite, the operation of which includes nitrogen-rich gas blanket, producing ample surface nitrogen in the graphite that corresponds to a more mobile C-14 inventory on the graphite surface [22]. New gas-cooled and molten salt cooled reactors are not planned to feature nitrogen-rich blankets; the distribution of radionuclide release-rates, then, represent a conservative, bounding estimate of radionuclide behavior in future irradiated graphite streams. Further details of the sampled values used to develop the release-rate distribution are found in Appendix C.

Uncertainty in the K_d values, similar to radionuclide release-rates, are modeled as a log-uniform distribution where minimum and maximum values are compiled from various sources for geochemical modeling in performance assessments (Table 3) [23, 24, 25]. For C and Cl, the relevant species are frequently assumed to be nonreactive tracer with a K_d value of 0 [26]. For these radionuclides, a minimum value of 10^{-10} m^3/kg is chosen to capture the nonreactive assumption within a log-normal distribution. Similarly, no sorption was credited for H-3, which was modeled with a single K_d of 0 [26].

Table 3. Kd values for analyzed radionuclides and soil types.

Radionuclide	**Distribution**	**Soil Type**	***Kd* (min, max) [m3/kg]**
H-3	Constant	All	0.0, 0.0
C-14	Log-Uniform	Silt	1.00E-10, 1.00E-3
		Sand	1.00E-10, 1.00E-3
		Clay	1.00E-10, 5.00E-3
Cl-36	Log-Uniform	Silt	1.00E-10, 9.00E-4
		Sand	1.00E-10, 1.00E-3
		Clay	1.00E-10, 9.00E-4
Ni-63	Log-Uniform	Silt	8.85E-1, 1.02E+0
		Sand	4.11E-1, 3.89E+0
		Clay	2.03E+0, 2.08E+0

A sensitivity analysis is conducted to determine which variables contributed most to the peak concentrations, using the variance-based Sobol sensitivity analysis, conducted using the following formula [17]:

$$\mathrm{SI}(\mathrm{X_i}) = \frac{\mathrm{var}[\mathrm{E}[\mathrm{Y_{peak}}|\mathrm{X_i}]]}{\mathrm{var}[\mathrm{Y_{peak}}]}$$

where X_i is i-th input parameter, Y_{peak} is the peak groundwater well concentration of the analyzed radionuclide, var[a] is the variance of a, E[$a|b$] is the expected value of a as a function of b and SI(X_i) is the sensitivity index describing the importance of X_i to the total variance of the output. This variance ratio is a measure of how much a particular parameter accounts for the variance compared to the total variance of the peak concentration. The computation is done through stochastic sampling of parameter sets, with the radionuclide transport model simulated for each parameter set. We use the approximation method developed by Wainwright et al. to compute $\mathrm{E}[\mathrm{Y_{peak}}|\mathrm{X_i}]$ using the 2nd order polynomial fit of the peak concentration as a function of X_i [28].

2.4 Reduced-Order Models for the Reactor-to-Repository Model Integration

The goal of the reduced-order models is to establish the relationship between the design parameters (i.e., nitrogen impurity and operational period) and the concentration limits, either in the waste (for waste classification) or in the groundwater well. This is done by the statistical regression based on the ensemble simulation data created in the UQ study (Section 2.3). Based on this statistical model, we can define the allowable parameter space and define the maximum combinations of operational time and nitrogen impurity, such that the irradiated graphite does not exceed a regulatory limit. We develop two reduced-order models; one for the LLW classifications (i.e., reactor simulation) and the other for the groundwater concentration (i.e., repository simulation). The combination of these two allow us to connect the design parameters and groundwater concentrations for the repository criteria.

We develop reduced-order models (ROM) for the reactor and repository simulations as a system of simplified functions that map variable material inputs to their respective simulation outputs. The ROMs allow both interpolation between a finite number of simulation executions to analyze a wider range of inputs as well as coupling between the reactor and repository ROMs to analyze irradiated graphite across its material lifetime in both reactor operation and repository disposal.

The reactor ROM analyzes the production of radionuclide inventory, specifically C-14, as a function of engineering parameters. Two parameters of interest are the nitrogen impurity of graphite, controlled during graphite fabrication, as well as the operation period, determined by the lifetime of graphite in a reactor system. The form of the relationship used to develop both reduced-order models is informed by two major pathways for C-14 production in HTGRs: the activation of C-13 in the bulk of graphite carbon, and the activation of N-14 impurities in the pores and surface of the graphite [29]. The result is a statistical model—i.e., the reactor ROM—that describes the concentration of C-14 as a function of nitrogen impurity and operational period described in Equation 1:

$$Q = \alpha_Q NT + \beta_Q T \tag{1}$$

where Q is the C-14 concentration of the activated graphite in Ci/m^3 , N is the approximate nitrogen impurity, and T is the operational period in years. α_Q is the linear coefficient describing N-14 activation to C-14, impacted by nitrogen impurity and operation period, and β_Q is the linear coefficient describing C-13 activation to C-14, impacted by operational period. Q can be compared with the LLW classes.

The reduced-order model for the repository model—i.e., the repository ROM—is the regression of the groundwater concentrations as a function of the source C-14 concentration Q. Because the groundwater concentration features considerable heteroscedasticity, with larger variation at larger source values, the regression is calculated between log_{10} of the inputs and outputs. The reduced-order model is described in Equation 2:

$$log_{10}(C) = \alpha_C \cdot log_{10}(Q) + \gamma_C \tag{2}$$

where C is the peak C-14 groundwater well concentration in pCi/L, Q is the source concentration of C-14 in graphite in Ci/m^3, α_C is the linear coefficient between source C-14 concentration and offsite C-14 groundwater well concentration, and γ_C is the fitting constant for the regression. C can be compared with GWPLs for repository compliance. Equations 1 and 2 can be combined to describe the coupled effects of the reactor source-term model and repository transport model on the resulting groundwater well concentration.

3. Results

3.1. Repository Assessment Results

We first simulate the radionuclide transport from the irradiated graphite waste from the 20-year operation of an MHTGR. To highlight the importance of parameters in a systematic manner, we have created three scenarios and computed resulting groundwater well concentrations (Figure 2): (1) instantaneous release without sorption/retardation, (2) instantaneous release rates with sorption/retardation, and (3) constant release rates crediting waste-form with sorption/retardation.

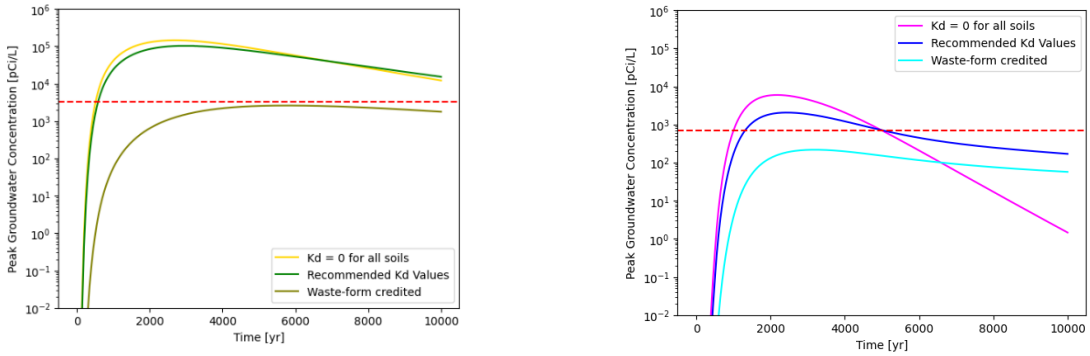

(a) (b)

Figure 2. Groundwater concentration over 10,000 years of (a) C-14 and (b) Cl-36 from irradiated MHTGR reflector disposed of in Clive LLW Repository. The red dotted line in each figure represents the GWPL for each radionuclide (3,200 pCi/L for C-14 and 700 pCi/L for Cl-36). All other radionuclides are calculated to have groundwater concentrations less than 1E-8 pCi/L over the 10,000 year period.

The resulting groundwater concentrations indicate that C-14, the most prevalent radionuclide in the irradiated graphite, also corresponds to the highest peak groundwater concentration at the well location. The C-14 concentration reaches a peak of 145,000 pCi/L at 2,800 years in the case of instantaneous release and no sorption, exceeding the GWPL by a factor of 45. The concentration decrease after the peak is associated with the radioactive decay of C-14. The inclusion of sorption decreases the calculated peak concentration by 29% to 102,000 pCi/L, still exceeding the GWPL by a factor of 32. In contrast, crediting the graphite waste form significantly reduces the peak concentration to 2,590 pCi/L, below the GWPL with a margin of 1.2. The peak concentration with waste-form credit also occurs later at 5,800 years.

Cl-36 is the second highest radionuclide concentration in groundwater, despite having a 151- and 113-times smaller inventory in the irradiated graphite compared to the first and second most prevalent radionuclide, C-14 and H-3, respectively. The shape of the breakthrough curve for Cl-36 is similar to C-14, with a peak at approximately 2000 years followed by decreasing concentrations, but for different reasons. The long half-life of Cl-36 of 301,000 years suggests that radioactive decay is an insignificant factor in groundwater concentration in the first 10,000 years. Instead, the higher maximum release rate modeled for Cl-36, two order of magnitude greater than C-14, results in a mobilization of a majority of the Cl-36 source within 2,000 years. Compared to the breakthrough curves for C-14, recommended K_d results in larger impacts on calculated peak concentrations. Including recommended K_d values for Cl-36 reduces calculated peak groundwater concentration by a factor of 3, from 5900 pCi/L to 2000 pCi/L. Crediting the graphite waste form results in a further reduction by a factor of 9 down to 220 pCi/L. Only Scenario 3 with the graphite waste-form credited results in Cl-36 groundwater concentrations below the GWPL, with a margin of 3.2.

3.2. Uncertainty Quantification Results

To systematically assess all the model parameters for performance, the Sobol sensitivity index is computed for each model parameter (Table 4 for Scenario 3). The sensitivity analysis considers two cases: (1) a fixed C-14 source concentration, and (2) a varying C-14 concentration from the five different graphite grades. For a fixed source, the release rate of C-14 has an outsized impact on its expected groundwater concentration, accounting for greater than 99% of the variance in the peak C-14 groundwater concentration. With the addition of a varied radionuclide source concentration, the radionuclide release rate is still calculated to account for 54.5% of the output variance, the greatest impact on the groundwater well concentrations. However, the radionuclide

source concentration accounts for 37.5% of the output variance, the second-most impactful parameter. The impact of the source concentration is considerable, given its variability compared to modeled release rate: The radionuclide source term varies over approximately 1 order of magnitude, while the release rate varies over 11 orders of magnitude.

Table 4. Sensitivity of Peak C-14 Groundwater Concentration to various model parameters for two cases: a constant C-14 source concentration from a single graphite grade and a varied C-14 source concentration from five graphite grades. Only the five greatest sensitivity indices are displayed

Parameter	Constant Source	Varied Source
C-14 Release Rate	9.92E-1	5.45E-1
Source Concentration	NA	3.75E-1
$Porosity_{Sand}$	5.45E-3	2.18E-2
Kd_{Silt}	6.17E-4	1.63E-2
Infiltration Rate	2.34E-4	1.47E-2

3.3 Reduced Order Predictive Model to Connect Reactor Design Parameters to the PA Criteria

The linear regressions between the C-14 source term and the calculated offsite C-14 groundwater concentration for cases 2 and 3 are depicted in Figure 6. For Case 2, where no waste-form is credited, the mean offsite C-14 groundwater concentration is greater than the GWPL for all graphite grades for all analyzed operational periods (Figure 3a). When the graphite waste-form is credited, several C-14 source terms are calculated to result in groundwater C-14 concentrations below the GPWL (Figure 3b). The graphed linear regressions also visualize the uncertainty in calculated offsite groundwater concentrations. In Case 3, with waste-form credited, the range of calculated groundwater concentrations nearly overlaps for each graphite composition. Additionally, the range of modeled groundwater concentrations for Case 2 without credited waste-form performance also shows considerable overlap between the different graphite compositions.

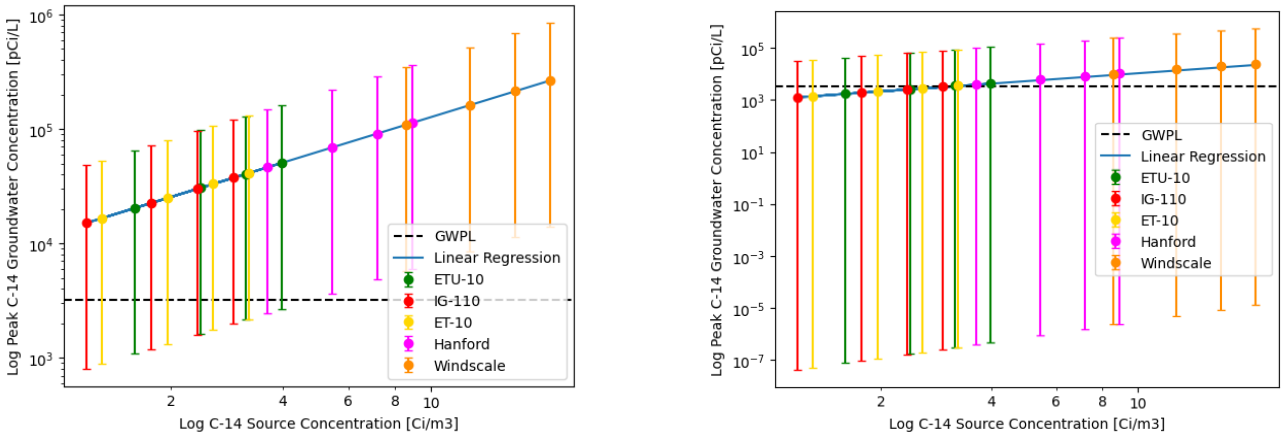

Figure 3. Peak C-14 groundwater concentration as function of C-14 source concentration for five graphite grades a) without waste-form credited, and b) with waste-form credited. Displayed data points correspond to the mean for each graphite composition at operational periods of 10, 15, 20, and 25 years

ROMs are developed to analyze the impact of design parameters, including the nitrogen impurity and operational period, on the resulting C-14 source concentration and its subsequent predicted groundwater well concentrations when disposed. The reactor ROM resulted in a nitrogen activation coefficient α_Q equal to 2.58E-2 and

a C-13 activation coefficient β_Q equal to 5.01E-2. While β_Q is greater than α_Q, the nitrogen activation term in Eq. 1 also scales with nitrogen impurity N. The values suggests that the activation of nitrogen impurities in graphite play the dominant role in the production of C-14 for impurities greater than 1.94 appm, below which C-14 production is predominantly from the activation of C-13 in the bulk graphite.

Two separate sets of C-14 transport parameters α_C and γ_C in Eq. 2 are calculated for the repository ROM: one for the case of instantaneous release of C-14 from the graphite, and one case where the graphite waste-form is credited. The instantaneous release case corresponds to $\alpha_{C,instant}$ equal to 1.27E4 and $\gamma_{C,instant}$ equal to 1.32E-2. γ_C nearly equals zero, suggesting a direct linear correlation in the log-space between source concentration and offsite groundwater concentration. The case with credited waste-form corresponded to lower values of $\alpha_{C,waste-form}$ and $\gamma_{C,waste-form}$ equal to 1.20E3 and -2.62E2 compared to the instantaneous case. The lower values reiterates that the incorporation of radionuclide release-rates reduce the calculated peak groundwater concentration of radionuclides.

Using the calculated coefficients, a parameter space can be defined for permissible nitrogen impurities and operational period. The permissible space is defined such that the C-14 concentration in the waste is below the limit for Class A and Class C waste, depicted in Figure 4a. The calculated combinations of operational period and nitrogen impurity fit squarely in the Class C envelope, with the exception of Windscale graphite composed of large nitrogen impurities. However, the envelope for Class A classification is projected to be difficult to attain, with maximum operational time of less than 14 years for all graphite grades examined.

Additional insights can be gleaned from combining the two reduced-order models for reactor and repository models, which is the regression between nitrogen impurity and operational period inputs and peak C-14 groundwater concentration output. The limit in this case is the GPWL for C-14 concentration in the offsite groundwater well. The result is depicted in Figure 4b for the case with waste-form credited. In the case without waste-form credit, the permissible envelope for compliance with GPWL are more restrictive compared to the LLW class criteria, such that the allowable parameter space is small. The reduced-order model suggests a maximum operational period of less than 6 years for 0 nitrogen impurity, an infeasible combination of parameters that precludes every graphite grade analyzed.

The allowable parameter space is expanded for the case in which the waste form is credited. For this case, modern nuclear graphite grades with nitrogen impurities between 2.5 and 5 ppm are predicted to result in offsite C-14 concentrations equal to the GWPL after 15-23 years of operation, a feasible parameter space for a facility operating for 40 years with one replacement of its graphite reflector.

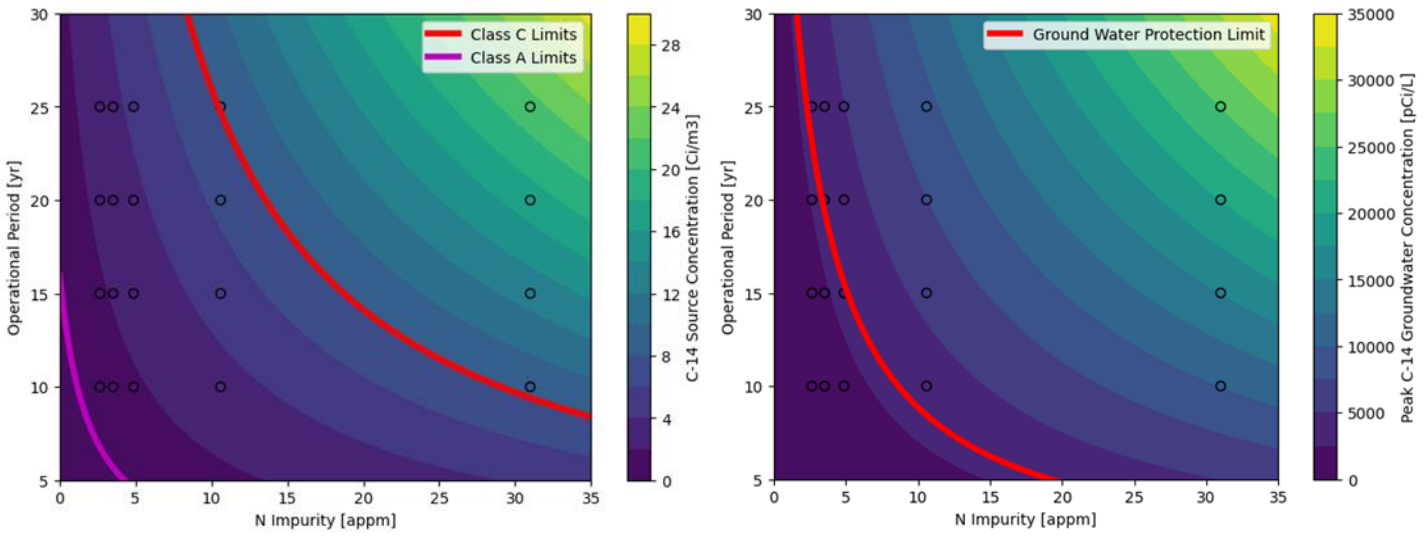

a) b)

Figure 4. a) C-14 source concentration and b) C-14 peak groundwater concentrations as a linear regression of operational period and nitrogen impurity of graphite. Displayed data points correspond to the mean for each graphite composition at operation periods of 10, 15, 20, and 25 years. Also depicted are the combination of each parameter that produces a) C-14 source concentration of 0.8 Ci/m3 (Class A limit) and 8.0 Ci/m3 (Class C limit) and b) C-14 groundwater concentration of 3,200 pCi/L (GWPL).

4. Discussion

The results show that the largest contribution to the offsite consequences would come from C-14, followed by Cl-36. This is attributed to the fact that C-14 constituted the greatest activity in the waste source term and hence contributed the greatest to offsite activity concentrations. Although H-3 has the second greatest inventory, and is similarly mobile in groundwater, the offsite concentrations of H-3 are negligible, owing to its short half-life. The difference among the radionuclides can be attributed to differences in sorption and solubility. For the radionuclides with relatively greater calculated groundwater concentrations, C-14 and Cl-36, the modeled K_d is significantly less than 1 and solubility is limitless. Ni-63, modeled as a chemical species with greater K_d and finite solubility, corresponded to smaller calculated groundwater concentrations.

In parallel, our results show that the graphite matrix offers an important constraint to offsite consequences. The realistic representation of radionuclide release through leaching or oxidation reduced the C-14 concentrations significantly compared to the instantaneous release scenario. In particular, crediting waste forms offers a viable route to enabling the graphite disposal at the Class A only site. At the same time, our sensitivity analysis has identified that the release rate is the dominant factor for the peak groundwater concentration. The large sensitivity to the release rate is partly attributed to the large parameter range associated with the large uncertainty in the measurements and data. The wide range of possible values—over 11 orders of magnitude—were selected from theoretical estimates of graphite oxidation in repository conditions and from measurements of radionuclide leaching from small samples of irradiated graphite in accelerated flow conditions [21, 20, 29]. The dependence of offsite groundwater concentration on waste-form performance for the radionuclides present in graphite indicate the need for further study of radionuclide leaching from irradiated graphite.

Our results are generally consistent with previous work to determine the consequences of graphite waste performance from existing and older reactors. The European Commission's CARBOWASTE project involved several studies examining the disposal of existing irradiated waste produced in several European countries [30]. Several of these studies, including analyses of irradiated graphite disposed in a theoretical UK geologic disposal facility, in the Saligny site in Romania, and in the Cigéo site in France, indicated that C-14 and Cl-36 would result in the greatest offsite consequences for graphite disposal. However, the different studies disagreed on whether C-14 or Cl-36 posed a larger risk. Additionally, studies as part of CARBOWASTE analyzed the ability of graphite waste-form to mediate radionuclide release. In the case of analyses of the possibility for future disposal of irradiated graphite in a theoretical Lithuanian geological repository, graphite leaching was included as a model feature. However, the examined release-rates featured a range of 5 orders of magnitude compared to this study's release rate that varied over 11 orders [30]. The Lithuanian study reached similar conclusions, that credit for graphite waste-form performance could significantly reduce predictions of radionuclide transport from the graphite waste, even if quantifying radionuclide release-rate included considerable uncertainty [30]. While the Lithuanian study analyzed the sensitivity of radionuclide transport on different values for release rate, this study offers a systematic sensitivity analysis of parameters in the performance assessment. The sensitivity analysis highlights the impact of release-rate uncertainty compared to other uncertain parameters in calculating offsite consequences of graphite disposal.

The feedback from the repository performance to the reactor design and operation is enabled by the model connections through reduced-order models (ROMs). The two separate ROMs are developed: one for the source term as a function of reactor parameters using reactor physics simulations, and the other for the peak groundwater concentration as a function of the source term and repository parameters using repository simulations. Once developed, the ROMs give insight into how the waste disposal considerations—satisfying the regulatory limits including WACs and GWPLs—can set the maximum limits for engineering design parameters, in the case of this study graphite nitrogen impurity and operational period. While our study considers a relatively simple case that couples a reactor design with limited parameters to one aspect of a performance assessment, the framework developed here opens the door for coupling more sophisticated ROMs that can represent reactor designs/operations and subsurface radionuclide transport [31, 32]. Such a modular framework allows technology designers and operators to make informed decisions considering the decommissioning and waste disposal constraints.

We would acknowledge that there are simplifications in repository modeling, with respect to the mobility of elements. Particular attention must be paid to C-14, modeled as highly mobile CO_2. Similarly, Cl is modeled as the highly mobile Cl^- ion. The choice to model C-14 as CO_2 and Cl as Cl^- are modeling conventions that offer worst-case conservative estimates for radionuclide transport that do not reflect the actual chemical

forms of these radionuclides in irradiated graphite waste. For Cl, in particular, previous studies have shown that analyzed irradiated graphite samples contain a significant portion of Cl as less mobile, organically-bound C-Cl [29]. The improved characterization of geochemical species and their transport parameters would be important to ensure that the associated risks of graphite disposal are accurately quantified.

5. Conclusion

In this study, we have developed a performance assessment model for disposing of irradiated graphite waste from advanced reactors in a LLW disposal facility. The novelties of our approach are: (1) the reactor/material parameters in the reactor physics models in Hines et al. (2025)—graphite impurity and operational time—are retained for the source terms in the radionuclide transport model, allowing direct connections between the reactors and repositories; (2) radionuclide release from the waste form is explicitly modeled, instead of instantaneous release; and (3) reduced-order models are developed to connect the reactor model results and the repository model, so that we can evaluate the reactor parameters to satisfy the repository performance criteria.

The performance assessment model simulates the radionuclide transport from graphite waste in a hypothetical near-surface low-level waste repository, quantifying the offsite groundwater concentrations. Mobile radionuclides such as C-14 and Cl-36 dictate groundwater concentrations with respect to the regulatory limit. In addition, the analyses of this study suggest that the potential risks posed by the high mobility of radionuclides present in graphite can be correctly represented by including the degradation of the graphite waste form and subsequent gradual release of radionuclides. In fact, the waste-form performance and radionuclide release rates are a dominant factor in predicting groundwater concentrations compared to other hydrological and geochemical parameters. By crediting the waste form, it is possible to dispose of irradiated graphite as the less expensive Class A waste compared to the Class C designation determined by the radionuclide source concentration. These methods offer potential for improving the practicality of managing not only irradiated graphite waste, but potentially other waste streams produced by new nuclear technologies.

Lastly, the study develops two separate ROMs: (1) a reactor model to calculate radionuclide production during graphite irradiation in a nuclear reactor and (2) a repository model to calculate radionuclide transport after graphite disposal in an LLW repository. The ROMs consider two important regulatory limits of C-14 for the disposal of graphite: the source concentration of C-14 for waste classification, and the offsite groundwater concentration of C-14 in the disposal assessment. By coupling the two ROMs, it is possible to create feedback from the repository criteria to reactor design parameters, such that we can determine the allowable range of reactor parameters (i.e., nitrogen impurity and irradiated for an operation period) to satisfy the repository regulatory limits for graphite disposal. The methodology developed here offers a novel approach for incorporating waste-disposal considerations into the initial design and operational planning of new nuclear reactors.

Acknowledgments

This work has been performed under DOE NEUP grant#DE-NE0009294. We would like to acknowledge Christina Leggett for providing the title “Design from Waste Up”. This study is also partially supported by the U. S. Department of Energy, under Cooperative Agreement Number DE-EM0005321 entitled ‘Consortium for Risk Evaluation with Stakeholder Participation (CRESP)’ awarded to Vanderbilt University, David S. Kosson, principal investigator. The opinions, findings, conclusions, or recommendations expressed herein are those of the authors and do not necessarily represent the views of the Department of Energy, Vanderbilt University, or the US Nuclear Regulatory Commission.

References

[1] Lee O. Nelson, “Optimum Reactor Outlet Temperatures for High Temperature Gas-Cooled Reactors Integrated with Industrial Processes,” INL/EXT-11-21537, 1017884, Apr. 2011. doi: 10.2172/1017884.

[2] L. Hines et al., “Graphite Waste Classification and Disposal Cost Estimation for High Temperature Gas and Salt Reactors To be published in: Annals of Nuclear Energy,” Annals of Nuclear Engineering, Aug. 2025.

[3] C. Mokoena and K. Shirvan, “Computational Framework for Estimating Cost of Equipment Disposal for Advanced Reactors,” *Nuclear Technology*, vol. 0, no. 0, pp. 1–17, doi: 10.1080/00295450.2025.2464424.

[4] International Atomic Energy Agency, "IAEA-TECDOC-1521: Characterization, Treatment and Conditioning of Radioactive Graphite from Decommissioning of Nuclear Reactors," International Atomic Energy Agency, Text, 2006. Accessed: Aug. 29, 2025. [Online]. Available: https://www.iaea.org/publications/7579/characterization-treatment-and-conditioning-of-radioactive-graphite-from-decommissioning-of-nuclear-reactors
[5] J. L. Everett and E. J. Kohler, "Peach bottom unit no. 1: A high performance helium cooled nuclear power plant," *Annals of Nuclear Energy*, vol. 5, no. 8, pp. 321–335, Jan. 1978, doi: 10.1016/0306-4549(78)90017-8.
[6] D. A. Copinger, D. L. Moses, and L. R. Cupidon, "Fort Saint Vrain Gas Cooled Reactor Operational Experience," NUREG/CR--6839, ORNL/TM--2003/223, 1495207, Jan. 2004. doi: 10.2172/1495207.
[7] M. Fisher, "IAEA-TECDOC-1043: Fort St. Vrain decommissioning project," in *Technologies for gas cooled reactor decommissioning, fuel storage and waste disposal*, Vienna: International Atomic Energy Agency, Sep. 1998, pp. 123–131. Accessed: Aug. 29, 2025. [Online]. Available: https://inis.iaea.org/records/52ewa-va380
[8] Nuclear Regulatory Commission, "PART 61—LICENSING REQUIREMENTS FOR LAND DISPOSAL OF RADIOACTIVE WASTE," NRC Web. Accessed: Jan. 25, 2023. [Online]. Available: https://www.nrc.gov/reading-rm/doc-collections/cfr/part061/full-text.html
[9] Nuclear Regulatory Commission, "Draft Environmental Impact Statement on 10 CFR Part 61 Licensing Requirements for Land Disposal of Radioactive Waste," NRC Web. Accessed: Jan. 18, 2023. [Online]. Available: https://www.nrc.gov/reading-rm/doc-collections/nuregs/staff/sr0782/index.html
[10] Nuclear Regulatory Commission, "Public Meeting on Integrated Low-level Radioactive Waste Disposal rulemaking," NRC Web. Accessed: Jan. 30, 2024. [Online]. Available: https://www.nrc.gov/pmns/mtg?do=details&Code=20231325
[11] J. Parnell, C. Brolly, and A. J. Boyce, "Graphite from Palaeoproterozoic enhanced carbon burial, and its metallogenic legacy," *Geological Magazine*, vol. 158, no. 9, pp. 1711–1718, Sep. 2021, doi: 10.1017/S0016756821000583.
[12] Nuclear Regulatory Commission, "10 CFR Part 63 -- Disposal of High-Level Radioactive Wastes in a Geologic Repository at Yucca Mountain, Nevada." Accessed: Jan. 30, 2024. [Online]. Available: https://www.ecfr.gov/current/title-10/part-63
[13] US EPA, "Guidelines for Evaluating and Adjusting the Post-Closure Care Period for Hazardous Waste Disposal Facilities under Subtitle C of the Resource Conservation and Recovery Act (RCRA)." Accessed: Jan. 23, 2024. [Online]. Available: https://www.epa.gov/hwpermitting/guidelinesevaluating-and-adjusting-post-closure-care-periodhazardous-waste-disposal
[14] L. Snead *et al.*, "Historic and modern nuclear graphite impurities: Pathways to improved waste strategies," *Current Opinion in Solid State and Materials Science*, vol. 39, p. 101242, Dec. 2025, doi: 10.1016/j.cossms.2025.101242.
[15] Nuclear Energy Agency, "Benchmark of the Modular High-Temperature Gas-Cooled Reactor (MHTGR)-350 MW Core Design Volumes I and II," 2017.
[16] UTAH DEPARTMENT OF ENVIRONMENTAL QUALITY DIVISION OF WASTE MANAGEMENT AND RADIATION CONTROL, "RADIOACTIVE MATERIAL LICENSE DRC-2024-007371." Aug. 2024.
[17] Energy Solutions, "UTAH LOW-LEVEL RADIOACTIVE WASTE DISPOSAL LICENSE - CONDITION 35 (RML UT2300249) COMPLIANCE REPORT." Jun. 01, 2011. Accessed: Jun. 08, 2024. [Online]. Available: https://documents.deq.utah.gov/legacy/businesses/e/energysolutions/depleted-uranium/performance-assessment/docs/2013/08Aug/ES6111DUPAReportDRCCompiled2113.pdf
[18] R. Kossik, "User's Guide GoldSim." GoldSim Technology Group, Oct. 2021. [Online]. Available: media.goldsim.com/
[19] International Atomic Energy Agency, "IAEA-TECDOC-2072: Managing Irradiated Graphite Waste," International Atomic Energy Agency, Text, 2024. Accessed: Aug. 29, 2025. [Online]. Available: https://www.iaea.org/publications/15272/managing-irradiated-graphite-waste
[20] United States Environmental Protection Agency, "Review of Geochemistry and Available Kd Values for Americium, Arsenic, Curium, Iodine, Neptunium, Radium, and Technetium," III, Jul. 2004. Accessed: Mar. 03, 2026. [Online]. Available: https://www.epa.gov/sites/default/files/2015-05/documents/402-r-04-002c.pdf
[21] B. P. van den Akker and J. Ahn, "Performance Assessment for Geological Disposal of Graphite Waste Containing TRISO Particles," *Nuclear Technology*, vol. 181, no. 3, pp. 408–426, Mar. 2013.
[22] A. A. Shiryaev, A. G. Volkova, S. Dvoryak, M. S. Nickolsky, and E. V. Zakharova, "Influence of long-term aqueous leaching of irradiated graphite on surface properties and behavior of radionuclides," *MRS Advances*, vol. 5, no. 3, pp. 177–184, Jan. 2020, doi: 10.1557/adv.2020.37.
[23] International Atomic Energy Agency, "IAEA-TECDOC-1616: Quantification of Radionuclide Transfer in Terrestrial and Freshwater Environments for Radiological Assessments," International Atomic Energy Agency, Text, 2009. Accessed: Aug. 29, 2025. [Online]. Available: https://www.iaea.org/publications/8103/quantification-of-radionuclide-transfer-in-terrestrial-and-freshwater-environments-for-radiological-assessments
[24] I. G. McKinley and A. Scholits, "A comparison of radionuclide sorption databases used in recent performance assessments," *Journal of Contaminant Hydrology*, vol. 13, no. 1, pp. 347–363, Jun. 1993, doi: 10.1016/0169-7722(93)90070-9.

[25] A. O. Pavlyuk, S. G. Kotlyarevskii, R. I. Kan, A. G. Volkova, and E. V. Zakharova, "Study of the Process of Leaching of Long-Lived Radionuclides 14C and 36Cl from Irradiated Graphite," *Radiochemistry*, vol. 63, no. 2, pp. 187–196, Mar. 2021, doi: 10.1134/S1066362221020090.
[26] S. C. Sheppard, M. I. Sheppard, J. C. Tait, and B. L. Sanipelli, "Revision and meta-analysis of selected biosphere parameter values for chlorine, iodine, neptunium, radium, radon and uranium," *Journal of Environmental Radioactivity*, vol. 89, no. 2, pp. 115–137, Jan. 2006, doi: 10.1016/j.jenvrad.2006.03.003.
[27] Utah Office of Administrative Rules, Ground Water Quality Protection. 2013. Accessed: Sep. 09, 2025. [Online]. Available: https://adminrules.utah.gov/public/rule/R317-6/Current%20Rules?
[28] H. M. Wainwright, S. Finsterle, Q. Zhou, and J. T. Birkholzer, "Modeling the performance of large-scale CO2 storage systems: A comparison of different sensitivity analysis methods," *International Journal of Greenhouse Gas Control*, vol. 17, pp. 189–205, Sep. 2013, doi: 10.1016/j.ijggc.2013.05.007.
[29] A.J. Wickham and D. Bradbury, "Graphite Leaching: A Review of International Aqueous Leaching Data With Particular Reference to the Decommissioning of Graphite Moderated Reactors," Electrical Power Research Institute, 1016772, May 2008.
[30] B. Grambow *et al.*, "Disposal Behavior of Irradiated Graphite and Other Carbonaceous Waste - Final Report," IGDTP, Apr. 2013. Accessed: Aug. 29, 2025. [Online]. Available: https://cordis.europa.eu/project/id/211333/reporting
[31] D. Price, M. I. Radaideh, T. Mui, M. Katare, and T. Kozlowski, "Multiphysics Modeling and Validation of Spent Fuel Isotopics Using Coupled Neutronics/Thermal-Hydraulics Simulations," *Science and Technology of Nuclear Installations*, vol. 2020, pp. 1–14, Jul. 2020, doi: 10.1155/2020/2764634.
[32] Y.-J. Wang *et al.*, "High Fidelity Digital Twin for Critical System Assessments," in *19th International Topical Meeting on Nuclear Reactor Thermal Hydraulics, NURETH-19, Brussels, Belgium*, 2022. Accessed: Dec. 26, 2025. [Online]. Available: https://www.researchgate.net/profile/Panagiotis-Tsilifis/publication/367635793_HIGH_FIDELITY_DIGITAL_TWIN_FOR_CRITICAL_SYSTEM_ASSESSMENTS/links/63d98c8864fc860638008357/HIGH-FIDELITY-DIGITAL-TWIN-FOR-CRITICAL-SYSTEM-ASSESSMENTS.pdf

Appendices

Appendix Radionuclide transport model through the vadose and saturated zones

The radionuclide transport model from the disposed waste through the vadose zone and saturated zone is described for the reference LLW site [ref]. We briefly describe it for the completeness. The key modeling parameters for each layer of the waste site are described in Table A-1.

Table A-1. Discretization scheme and material description for 1-D radionuclide transport model along the pathway from the disposal system to the unsaturated zone, and then to the saturated zone

LLW Site Layer	Thickness [ft]	Material	Mean Porosity	Mean Hydraulic Conductivity [cm/s]	Bulk Density [g/cm3]
Waste Layer	16.2	Silt	0.39	5.14E-5	1.609
Clay Liner	0.61	Clay	0.43	5.16E-5	1.516
Unsaturated Zone	4.57	Silt	0.39	5.14E-5	1.609
Saturated Zone	4.57	Sand	0.29	9.60E-4	1.566

The flow in the unsaturated layers is influenced by rain infiltration, layer saturation, and soil hydrology. To account for these mechanisms and quantify the downward flux, the developed model implements a first-order

numerical solution to the Darcy flow equation for water flux in the unsaturated media [17]: In this model, the 1-D water flux is fixed as constant through the layers, preserving mass:

$$\frac{dh}{dz} = \frac{q}{K_L(h)} - 1 \tag{A.1}$$

Where h is the hydraulic head; z is the depth, q is the water flux, a fixed constant sampled from site meteorological data [17]; and K_L is the hydraulic conductivity. The finite element solution for h takes the following form:

$$h_{n+1} = h_n + \frac{k_1+k_2}{2} \tag{A.2}$$

Where k_1 and k_2 are projections for the gradient of the hydraulic head developed from a second-order Runge-Kutta solution to the Darcy Equation [17] for accommodating the heterogeneous properties:

$$k_1 = \Delta z\left(\frac{1}{K_L(h_n)} - 1\right) \tag{A.3}$$

$$k_2 = \Delta z\left(\frac{1}{K_L(h_n+k_1)} - 1\right) \tag{A.4}$$

The numerical solution implements the Mualem model for K_L depending on the soil moisture θ and hydraulic head h [17]. The water retention curve is defined as:

$$\theta = \theta_r + (\theta_s - \theta_r)\left(\frac{h}{h_b}\right)^{D-3} \tag{A.5}$$

Where θ_s is the saturated water content, θ_r is the residual water content, h_b is the air entry pressure head, and D is the soil fractal dimension. The Mualem model for hydraulic conductivity is implemented as [17]:

$$K_L = K_S\left(\frac{\theta-\theta_r}{\theta_s-\theta_r}\right)^{-\left(\tau+\frac{2}{D-3}\right)} \tag{A.6}$$

Where K_S is the static hydraulic conductivity and τ is the Mualem empirical parameter. All of the variables are constant or determined by the soil type, depicted in Table A.2. For each soil type, the statistical ranges of parameters are defined. Assuming the zero hydraulic head and full saturation conditions at the lowest cell of the unsaturated zone, the Runge-Kutta solution could be applied sequentially up through the layers, quantifying the hydraulic head at each cell. Then the hydraulic gradient is converted to the downward flux of water and radionuclide velocity.

Table A.2. Parameters for hydrology model in unsaturated layers of 1-D radionuclide transport model [17]

Region	K_S **[cm/s]**	h_b **[cm]**	θ_s	θ_r	D	τ
Waste Layers	(5.14E-5, 5.95E-6)*	(8.85E0, 9.29E-1)	(3.93E-1, 6.11E-1)	(6.78E-3, 2.05E-3)	(2.73E0, 5.21E-3)	2
Clay Liner	(5.16E-5, 5.97E-7)	(1.04E2, 1.72E0)	(4.28E-1, 6.08E-3)	(8.95E-4, 1.08E-1)	(3.01E0, 9.93E-5	2
Silt Below Liner	(5.14E-5, 5.95E-6)	(8.85E0, 9.29E-1)	(3.93E-1, 6.11E-1)	(6.78E-3, 2.05E-3)	(2.73E0, 5.21E-3)	2

*(a, b) read as Normal distribution with mean a and standard deviation b

In the saturated zone, the horizontal advective transport is modeled to determine the maximum radionuclide concentration in a monitoring well 73 m from the site. The saturated zone modeling involves two regions: 25 cells under the waste cell's footprint and 20 cells connecting the waste cell footprint to the offsite well, which are the same as the original model [ref]. We note that this grid cell size determines the dispersion of contaminants. A constant hydraulic gradient is assumed for the lateral flow, allowing a simple arithmetic solution to the Darcy flux equation. Parameters for the saturated zone are provided in Table A.3

Table A.3. Parameters for hydrology model in saturated layers of 1-D radionuclide transport model [17]

Variable	Distribution	mean	σ
Ks [cm/s]	Normal	9.6E-4	9.67E-5
dh/dl	Normal	6.94E-4	1.27E-4
porosity	Normal	0.29	0.05

Appendix B Benchmark of LLW Performance Assessment

For benchmarking, our repository model simulates the same radionuclide inventory corresponding to depleted uranium in a LLW repository in the Western US [17]. Particular attention is paid to the calculated groundwater concentrations of Tc-99 and I-129, as these were the most mobile species in the reference PA. The mean of the offsite peak groundwater concentration from 5000 simulations for both radionuclides after disposal at 5 m below waste cover for 500 years are displayed in Table B.1.

Table B.1. Benchmark of Mean Peak Groundwater Concentrations for radionuclides disposed of in LLW Repository for 500 years at a disposal depth of 5 m [17].

Radionuclide	Reference PA Mean Concentration [pCi/L]	Study PA Mean Concentration [pCi/L]
Tc-99	437	436
I-129	0.368	0.102

For Tc-99, the peak groundwater concentration calculated by the study's PA almost exactly aligns with the one calculated in the reference PA. For I-129, the peak groundwater concentration calculated by the study's PA differs by a factor of 3.6; while not as closely aligned with the results of Tc-99, the peak groundwater concentration of I-129 calculated agrees in magnitude with the result from the reference PA. The alignment between the calculated peak groundwater concentrations between the study's repository model and the reference PA suggests that simplifications made in developing the study's model, including the omission of effects including erosion and lake reformation, will have limited impact on the focus of peak groundwater concentrations.

Appendix C Survey of Graphite Leach rates and oxidation rates

To develop the distribution to model radionuclide release from graphite, studies in graphite leaching and oxidation were surveyed for theoretical and experimental values. The spectrum of C-14 release-rates reviewed for this study are presented in Figure C.1. The wide range of release-rates account for qualitatively different mechanisms for radionuclides in graphite to become mobile in the groundwater environment. At the lowest end are theoretical values for graphite oxidation, which have been applied to analyze the degradation of matrix

graphite in TRISO fuel forms disposed in Yucca Mountain [21]. At the highest end are experimental results of graphite leach tests for small pieces of irradiated graphite from decommissioning facilities [30].

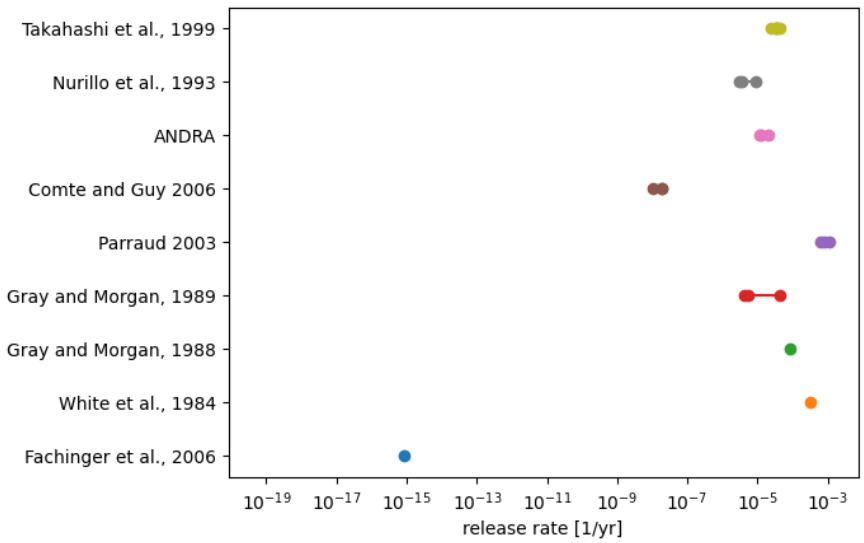

Figure C.1. Surveyed values of C-14 release rates including theoretical model of homogenous release via graphite oxidation and multiple empirical leach studies of irradiated graphite [21, 29].

Appendix D Groundwater Transport and Parameter Sensitivity Comparison for Ni-63

To further evaluate the impact of K_d, we analyze Cl-36 and Ni-63 concentrations in the liner below the waste cell after 1,000 years, because high-K_d radioactive species are found not to penetrate to groundwater. The shorter distance and timespan are chosen to include Ni-63 in the analysis, which has a shorter half-life and greater K_d compared to C-14 and Cl-36. The calculated sensitivity indices for Cl-36 and Ni-63 are described in Table D-1. The significance of release-rate is demonstrated to be similarly significant for Cl-36, a radionuclide nearly as mobile as C-14 as the modeled Cl^- species. The greater relative impact of K_d can be explained in part by the shorter spatial domain examined by the comparison case. However, for less-mobile radionuclides such as Ni-63, K_d contributed significantly more to the variance of the resulting concentration. The K_d value in silt for Ni-63 contributed slightly more to the variance of the concentration than the release-rate, despite the similarly wide range of release-rates sampled from as other radionuclides.

Table D-1. Sobol sensitivity index of peak radionuclide concentration for Cl-36 and Ni-63 in waste cell linear for various model parameters. Concentrations are calculated for repository liner during 1000-year period due to short lifetime of Ni-63

Parameter	**Cl-36**	**Ni-63**
Release Rate	9.46E-01	2.57E-01
Kd_{Silt}	5.39E-02	2.73E-01
Kd_{Sand}	1.05E-05	1.89E-01

The impact of release rates is illustrated by the calculated concentration plotted against the release-rate, depicted in Figure D-1. For C-14, a sharp linear trend is observed between concentration and release-rate. A similar linear trend is found for C-36, although the wider spread indicates the greater influence of other variables including K_d. For Ni-63, the positive trend between release-rate and concentration is apparent, but the wider

spread around the trend-line suggests the greater significance of other parameters, specifically K_d for the site soils.

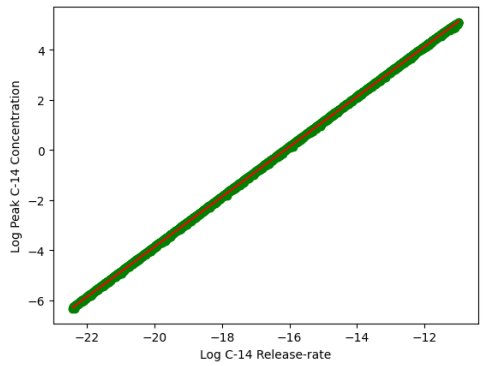

a)

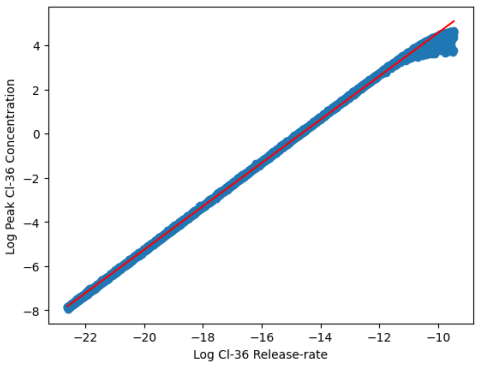

b)

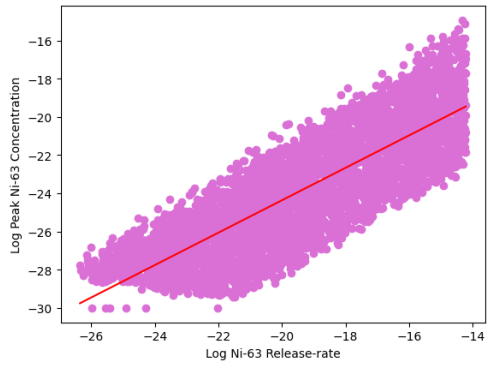

c)

Figure D-1. Peak radionuclide concentration in waste cell liner comparison case for a) C-14, b) Cl-36, and c) Ni-63 compared to release-rate of radionuclides. The red line in each graph depicts a linear regression of all simulated data points.